Elucidation of a lingual detection mechanism for high-viscosity solutions in humans

Journal:	*Food & Function*
Manuscript ID	FO-ART-07-2021-002460.R1
Article Type:	Paper
Date Submitted by the Author:	21-Oct-2021
Complete List of Authors:	Miles, Brittany; The Ohio State University, Food Science and Technology Wu, Zhenxing; The Ohio State University, Otolaryngology Kennedy, Kelly; The Ohio State University, Oral & Maxillofacial Surgery and Dental Anesthesiology Zhao, Kai; The Ohio State University, Department of Otolaryngology-Head and Neck Surgery Simons, Christopher; The Ohio State University, Food Science and Technology

SCHOLARONE™
Manuscripts

Elucidation of a lingual detection mechanism for high-viscosity solutions in humans

Brittany L. Miles[1], Zhenxing Wu[2], Kelly S. Kennedy[3], Kai Zhao[2], and Christopher T. Simons[1*]

[1] Department of Food Science & Technology, The Ohio State University, 2015 Fyffe Rd., Columbus, OH 43210-1007

[2] Department of Otolaryngology – Head & Neck Surgery, The Ohio State University, 915 Olentangy River Rd., Columbus, OH 43212-3153

[3] Division of Oral & Maxillofacial Surgery and Dental Anesthesiology, The Ohio State University, 305 W. 12th Avenue, Columbus, OH 43210-1267

*To whom correspondence should be addressed:

Christopher T. Simons Ph.D.
The Department of Food Science & Technology
The Ohio State University
2015 Fyffe Rd., Columbus, OH 43210-1007
Tel: 614-688-1489
Fax: 614-292-0218
Email: simons.103@osu.edu

Abstract

While perception of high-viscosity solutions ($\eta > 1000$cP) is speculated to be linked to filiform papillae deformation, this has not been demonstrated psychophysically. Presently, just-noticeable-viscosity-difference thresholds were determined using the forced-choice staircase method and high-viscosity solutions ($\eta = 4798$-12260cP) with the hypotheses that the tongue would be chiefly responsible for viscosity perception in the oral cavity, and that individuals with more, longer, narrower filiform papillae would show a greater acuity for viscosity perception. Subjects (n=59) evaluated solutions in a normal, "unblocked" condition as well as in a "palate blocked" condition which isolated the tongue so that only perceptual mechanisms on the lingual tissue were engaged. Optical profiling was used to characterize papillary length, diameter, and density in tongue biopsies of a subset (n=45) of participants. Finally, psychophysical and anatomical data were used to generate a novel model of the tongue surface as porous media to predict papillary deformation as a strain-detector for viscosity perception. Results suggest that viscosity thresholds are governed by filiform papillae features. Indeed, anatomical characterization of filiform papillae suggests sensitivity to high-viscosity solutions is associated with filiform papillae length and density (r=0.68, p<0.00001), but not with diameter. Modelling indicated this is likely due to a reciprocal interaction between papillae diameter and fluid shear stress. Papillae with larger diameters would result in higher viscous shear stress due to a narrower gap and stronger fluid-structure interaction, but a larger-diameter papilla would also deform less easily.

Introduction

Oral tactile sensitivity enables important physiological and behavioral functions including food texture perception, bolus formation, swallowing, and speech. Food texture perception specifically, provides relevant information about a food's identity[1] and suitability for consumption [2]. Food texture is, therefore, a proximal determinant of food choice and intake [3]. Despite the inarguable importance of oral mechanosensation, the mechanisms underpinning this process are not well characterized. While previous studies have indicated the tongue plays a prominent role in texture perception, little work has been done to characterize the tissue-specific mechanisms involved[4-6]. Recent evidence in mice[4] and humans[5] has shown peripheral mechanosensory endings of the tongue to be different from those in other, highly-tactile tissues including glabrous skin [6] whereas the mechanosensory afferent neurons innervating these different tissues display remarkable similarity in terms of receptive field size, adaptational properties, the proportions of different afferent types, and their action potential responses to standardized stimuli [7,8]. Even still, the presence of specialized structures—filiform and fungiform papillae—on the lingual surface further differentiates these tissues and suggests mechanisms underpinning food-related texture perceptions may be distinct from those enabling texture discrimination in skin.

Viscosity is an important and relevant attribute in liquid and semisolid food product categories. It has been linked to a variety of textural attributes including positive attributes such as creaminess, and negative attributes such as sliminess and mushiness [9–11]. Yet, the perception of viscosity, like perception of many other textural cues, is not well understood. Prior studies on viscosity perception can be broken into two main categories: those focused on relating physical increases in viscosity to perceived increases in thickness [12–14] and those comparing oral viscosity evaluation to other evaluation methods (i.e. stirring, pouring, etc.) [10,15]. However, the mechanism driving viscosity perception in the oral cavity, or how individual variation may impact this process, remains unknown.

Viscosity perception in the oral cavity involves a variety of structures, but which structures are involved and how they are utilized is likely a function of the viscosity of the solution. While thinner solutions' (η=0-100cP) perceived thickness is generally based on their passage rate through the mouth during swishing or their spontaneous spread over the tongue, thicker solutions (η>1000cP) are almost exclusively evaluated by the pressing of the tongue against the hard palate [11,16,17]. The bulk of the solutions evaluated in previous psychophysical studies are also primarily thinner solutions (η<1000cP) [10,12–15]. Thus, the findings from these studies, often gathered via the aforementioned swishing method, may have limited applicability in higher-viscosity systems which rely on a different evaluation technique [10,12,13].

Filiform papillae are ubiquitous, covering the majority of the anterior two-thirds of the dorsal tongue surface. Despite this, functional studies in humans are missing and the role of these structures has yet to be clearly established. Mathematical modeling studies have posited a potential role for filiform papillae in the perception of "high-viscosity" solutions. While largely theoretical, these studies suggest the idea that filiform papillae act as strain amplifiers in response to viscous solutions flowing across the tongue's surface in turn causing a directional deformation of those structures[16,18]. The papillae may be of such importance that their presence causes an increase of strain in response to a viscous solution by an order of magnitude relative to a surface without the structures[18]. This directional deformation is postulated to then transduce a signal to the brain either via specialized mechanoreceptors inside the papilla structure or via a sublingual receptor responding to strain on the surface[5,16,18,19]. While the density of the other papillary structure found on the apical tongue, the fungiform papilla, has been linked to perception acuity of other textural percepts, this study seeks to specifically characterize the role of the filiform papillae in texture perception[20,21], Although these structures have long been speculated to be involved in mechanosensation, no psychophysical studies have been completed confirming their role.

Human filiform papillae are a complex comprised of up to 30 hair-like projections off of one papillary body, although the body and hairs are thought to act as a single unit [22–24]. Recently, these structures were confirmed to contain specialized mechanosensory endings, with each one containing one to several end bulbs of Krause, free, myelinated nerve endings, and a subepithelial nerve plexus presumed to be somatosensory [5]. Unfortunately, while studies appear to be in agreement about the general location of the papillary structures on the tongue, reports of the papillae's length (anywhere from 250μm to 2-3mm), diameter (100μm to over 450μm), and assumptions on their elasticity (2.6-25kPa) vary greatly[16,18,19,23,24]. This variation in turn leads to multiple proposed viscosity cut-offs for when these structures may become relevant for perception. For thinner solutions (η<100cPs), these structures are likely irrelevant as these solutions do not generate enough force to lead to deformation. Most conservatively though, van Aken (2010) proposed that a minimum viscosity of 1000cP was needed to activate the papillary deformation mechanism of perception.

Taking this information together, we arrive at three primary objectives for this study. First, characterize the perception of high-viscosity solutions in the oral cavity via psychophysical testing. Second, investigate the proposed papillary mechanism of perception to determine what role anatomical variation in papillary attributes may be playing in viscosity perception. By correlating papillary traits to psychophysical performance, we can assess not only the role the structures may generally play, but also how individual variation in these structures may influence viscosity perception. Finally, we utilize these anatomical and perceptual data to model the filiform papillae deformation as a function of shear stress to predict viscosity sensitivity. To this end, we adapted our model that treats the human tongue surface as a porous material[25] to drastically simplify computational complexity. We hypothesize that filiform papillae on the tongue act as strain amplifiers to viscous shear and therefore, viscosity sensitivity will be predicted based on the filiform papillary attributes of length, diameter, and density.

Materials and Methods

Stimuli

Stimuli consisted of nine glycerol/water/carboxymethyl cellulose (CMC) solutions; one reference solution ([CMC]=1.125% w/v, $\bar{\eta}$ =5068cP ± 270cP) and eight variable solutions ([CMC] = 1.1538%-1.5% w/v, $\bar{\eta}$ =5507cP-11840cP ± 321cP). A minimum viscosity of 1000cP across the potential evaluation shear rates ($10-50s^{-1}$) was used to ensure all solutions could be evaluated via the proposed papillary deformation mechanism. Variable solutions increased in concentration of CMC in 0.03125% w/v increments. All solutions were made with a 55:45 reverse osmosis (RO) water (0.0001µm pore size)/glycerol solution. Glycerol (Essential Depot, Inc., Sebring, FL) was utilized in this mixture due to its known synergistic thickening with CMC (Sigma-Aldrich Corp., St. Louis, MO) [26]. Solutions were stored in sealed, plastic containers at ambient temperature (20-23°C) before being portioned out into 10mL syringes outfitted with 2cm of flexible, Tygon® tubing (Saint-Gobain Performance Plastics, Courbevoie, France), for testing.

Subjects

59 participants (age 19-40, 18M/41F) were recruited via the Ohio State University Consumer Sensory Database. Individuals completed a pre-test screener (Qualtrics, Provo, UT) including questions on age, physical limitations, food allergies or sensitivities, smoking status, and presence of oral diseases. The age range for recruitment was restricted to the ages of 18-40 to limit any potential decreases in acuity attributable to age [20,27]. Individuals with a self-reported history of an oral disease, food allergies or sensitives, mobility problems that would prevent them from completing the physical task, as well as smokers, were excluded. Subjects were instructed not to eat or drink for one hour prior to testing. Each subject completed the psychophysical testing individually during two, one-hour sessions one week apart. After completion of psychophysical testing, subjects underwent the biopsy protocol. Biopsies were completed by a board-certified oral and maxillofacial surgeon. Biopsies were taken between 4-14 days after the last psychophysical testing session. Subjects were compensated $70 for their participation in the study. All parts of this study were approved by the Ohio State University Institutional Review

Board (2013B0277, psychophysical protocol and 2018H0509, biopsy protocol). Data was collected under the written and informed consent of each subject.

Viscosity Discrimination

Viscosity discrimination ability was determined using the forced-choice, up-down staircase method to assess participants' Just-Noticeable-Difference (JND) threshold for viscosity [28,29]. Previous studies have found that high-viscosity solutions (>1000cP) are evaluated at shear rates between 10 s^{-1} and 50 s^{-1} [11,30]. Thus, for the stimuli used here, the solutions were created with the goals of being odorless and tasteless and having recorded viscosities above 1000cP over the 10-50s^{-1} range. Discrimination ability was evaluated in an Unblocked (UB) condition and a Palate-Blocked (PB) condition (see Figure 1A-B). Physical barriers, as opposed to topical numbing agents, were used due to the challenges of achieving complete numbing of this tissue seen previously [31]. Similar mouthpieces have been used in this situation to allow for the independent assessment of the sensitivity of the tongue[31,32]. By so doing, any contribution of the hard palate to viscosity perception is eliminated including any potential amplification mechanism resulting from interactions between the filiform papillae and rugae. For a detailed explanation of the mouthpiece creation, see Supporting Information. Each evaluation occurred during one of the two sessions, one week apart. The order of these conditions was randomized and counterbalanced across participants.

During the first psychophysical session, participants completed the informed consent and a brief demographic questionnaire before molding their PB mouthpiece. Prior to both sessions, participants would rinse with a concentrated Gymnema leaf extract solution (Bio-Botanica, Inc., Hauppauge, NY) made with 2mL of extract (~1200mg of gymnemic acid) and 6mL of RO water for one minute before expectorating the solution. Gymnemic acids from the Gymnema plant have been shown to inhibit the perception of sweetness [33]. This rinse was done to help block any sweetness imparted by the glycerol in the test solutions. While the solutions were theoretically

isointense in terms of sweetness (as all solutions contained the same proportion of glycerol to water), rinsing helped to ensure the perceivable difference between the solutions was viscosity.

Participants were seated in a dental chair and blindfolded to prevent solution discrimination based on visual cues. Participants then evaluated pairs of solutions one of which was always the reference solution and another, variable solution. One at a time, 0.5mL of the solution was applied to the dorsal medial tongue (approximately 2cm back from the tongue tip), and the participant would press the applied solution upward against the rugae of the palate three times before the solution was removed by the participant by gently blotting with KimWipes (Kimberly-Clark, Irving, TX). Participants were instructed to avoid dragging the tongue forward and backward or laterally to help standardize oral movement during evaluation and limit salivary incorporation. Preliminary testing with a subgroup of subjects found this area of the tongue and this specific manipulation to be routinely used by most individuals when assessing the viscosity of very thick solutions. Wiping was used instead of expectorating or swallowing to minimize cues coming from the lips or esophagus, respectively. Solution evaluation was completed using the forced-choice staircase method described previously (see Miles et al., Section 2.2.2) and comparisons were carried out until eight reversals were achieved [34]. Solution presentation order (reference vs. variable solution) was randomized and counterbalanced across the trials. In the blocked evaluation condition, the evaluation protocol was the same as in the UB condition, however, participants were instructed to press the solutions against the plastic mouthpiece.

Lingual Biopsy

Biopsies were completed in the Department of Oral and Maxillofacial Surgery at the Ohio State University's College of Dentistry by a board-certified oral and maxillofacial surgeon. After obtaining surgical consent and acceptable vital signs, participants' tongues were isolated and retracted by a surgical assistant while local anesthesia was administered by the surgeon. 1.8ml of 2% lidocaine with 1:100,000 epinephrine was locally infiltrated at the surgical site. After 5 minutes had passed and vasoconstriction was visualized, the tongue was again isolated and retracted for

the biopsy procedure. A 5mm biopsy punch was used to incise through mucosa and submucosa

in the middle third of the dorsal tongue to the right of the midline, and tissue was removed using

forceps and scissors. The wound was then closed primarily with 3-0 chromic gut suture. Once

removed, the biopsied tissue was placed in a neutral phosphate-buffered 20% formalin solution at

20°C. Samples were stored in the fixing solution at 4°C for one week, prior to anatomical

characterization. Care was taken to standardize the duration of time samples spent in the fixative

to help minimize inter-individual variation in tissue shrinkage across subjects, however it is likely

that some shrinkage did occur in all samples during the storage time.

Lingual Anatomical Characterization

To identify structural variance in the population to relate to performance, it was necessary

to find a method for characterizing filiform papillae in humans. While the non-invasive Denver

Papillae Protocol is often used to quantify fungiform papillae size and density, the method lacks

the consistency and detail necessary for quantifying variations in attributes of the filiform papillae

such as average papilla height, diameter, and density [35]. While scanning electron microscopy

(SEM) has been successfully used to characterize variation in papillae previously, this method is

time consuming, requiring a minimum of 48 hours to prep tissue, and is generally destructive

[24,36,37]. Instead, a novel method for the evaluation of papillary variance, optical profiling, was

completed using a Keyence VK-X210 Laser scanning confocal microscope (LSCM) (KEYENCE,

Osaka, Japan). For more background on optical profiling see Supporting Information.

Anatomical characterization was completed for a subset of participants (n=44) (Figure

2A&B). Remaining participants were excluded either due to a failure to attend the biopsy session

(n=4), or due to blood present on the surface of the sample during fixing (n=10) preventing the

surface structures from being sufficiently visualized. Biopsied samples were removed from the

fixative and rinsed with DI water before imaging. Eight images were taken across each sample

using 10x optical zoom minimizing overlap between the images. While the majority of the

samples contained only filiform papillae, a subset of the samples (n=5) did have at least one

fungiform papilla present. To ensure accurate density measurements, all images taken excluded the fungiform structures.

Papillary data were analyzed using Keyence Multifile Analyzer software (KEYENCE, Itasca, IL). All samples were corrected for surface tilt and curvature. Papillary lengths and diameters were determined using the profile tool to draw segments from the base to tip of papillae, parallel or perpendicular to the direction of the papillary body, respectively (Figure 2B). Papillary diameter was measured by taking the 2pt distance between the edges of the papillae, Papillary diameter was measured at both the base and the tip of the papillary structures. Length measurements were taken by measuring the segment length of the surface profile (as opposed to the absolute distance along the X and Y planes), which factored in distance in the Z plane. Three length, base diameter, and tip diameter measurements were taken per image. Papillary density was calculated by visually identifying the number of papillae present in an image (Figure 2B). Using the plane tool, density was determined by dividing the count data by the area as calculated by the XY-measure function. For a detailed explanation and example measures see Supporting Information and Figure S1A-E.

Data Analysis

Average viscosity JND was analyzed using a paired samples t-test in IBM SPSS Statistics 26 (IBM, Armonk, NY). To analyze papillary data, values were averaged across images to determine an average papillary length, diameter, and density for each individual. Papillary attributes were then correlated to PB JND using a linear model ($\alpha=0.05$). Additionally, a multiple, linear regression was used to determine the impact of the average measured papillary attributes of length, diameter, and density, as well as demographic information including age and sex on PB JND. The multiple regression model was executed in a stepwise fashion, removing attributes that did not meet the criteria for inclusion ($p \geq 0.100$). All data are reported as averages ± standard error.

Model Generation

After gathering and analyzing the papillary data, we used this information to generate a novel model of viscosity perception on the tongue. Unlike the theoretical models discussed earlier, this new model utilized a porous media approach to connect individual anatomical variations to JND data[16,18]. Porous media are extensively studied in industrial engineering and can significantly simplify the computational processes of modeling fluid flow through a porous material, where modeling the exact flow through each pore is challenging to impossible[25]. Instead, the system is modeled via key material properties: the *porosity*, or the average proportion of the material that is empty (i.e., the volume of space through which the fluid can flow) and the *permeability*, or the ease of which a fluid can pass through the material. For a complex structure through which a viscous fluid flows, such as the tongue surface with numerous papillary structures, the porous model approach is ideal for the computational purpose.

In the model simulation, measured filiform papillary properties from each subject including the length, diameter (dp) at the tip and the base, and the distribution density (Dp), was used to calculate the shear stress exerted onto the tongue surface and papilla structure by the viscous solution. The key parameters of the porous medium—permeability and porosity— were estimated based on well-established theoretical formulae[38–40]. Other structures, including fungiform papillae, may also potentially contribute to the effective porous structure of the lingual surface[16,18]. However since fungiform papillae are much less numerous than filiform papillae, incorporating their contribution into the porous media model would only slightly modify the material properties (see[16,18]). In addition, few biopsies contained fungiform papillae from which biometric measurements could be obtained. As such, incorporating fungiform parameters into the model would require the use of standard reference values for all subjects, and individual variability would not be accounted for. Thus, using the filiform papillary data, the direct volume method was used to obtain the porosity[40]:

$$\varepsilon = 1 - \frac{V_s}{V_t},$$
(1)

where V_s is the solid volume of the human tongue surface region and V_t is the total volume of the region. The permeability (K_p) depends on both its morphology and its porosity. We applied a published empirical formula, adapted for porous fiber[38,39]:

$$\frac{K_p}{r_f^2} = \frac{1}{8(1-\varepsilon)}\left(-\ln(1-\varepsilon) - 1.476 + 2(1-\varepsilon) - 1.774(1-\varepsilon)^2 + 4.076(1-\varepsilon)^3\right), \qquad (2)$$

where r_f is the average radius of papillae and ε is the porosity of the predicted porous media.

We next considered a fully developed, incompressible flow driven by a constant pressure gradient $dp/dx < 0$ between two parallel surfaces (Figure 3A). The top surface is the hard palate/plastic divider used in the experiment. The bottom surface is the tongue surface covered with a, homogenous, isotropic porous medium. The gap between the two surfaces is *2L+2H*, where *2H* is the thickness of a porous medium (the tongue surface) and *2L* is the height of the viscous flow region (between the hard palate/plastic divider and tongue surface). The plastic divider was made of a hydrophobic polyester thermoplastic which may have impacted the velocity profile close to its surface[41]. However, in the present study, our focus was on the flow near the tongue surface, which is relatively far from the plastic mouthpiece, and the effect of the hydrophobic phenomena was, therefore, negligible. The *x*-axis and *y*-axis are directed along and normal to the flow, respectively and the origin is located at the fluid-porous interface.

The momentum of the flow in the free-flow region was solved by using the incompressible Navier-Stokes equation

$$\mu\frac{d^2u}{dy^2} - \frac{dp}{dx} = 0, \qquad y \in [0, 2L] \qquad (3)$$

where u represents the velocity in the channel, p is the pressure, and μ is the dynamic viscosity, respectively. Additionally, the Reynold's number is very small (Re<1) due to the high viscosity flow and the microstructure of the tongue surface, thus the flow is considered to be laminar.

The Brinkman's equation was used as the governing equation in the porous medium region[42]:

$$\frac{\mu_e d^2 u_m}{\varepsilon \, dy^2} - \frac{\mu}{K} u_m - \frac{dp}{dx} = 0, \quad y \in [-2H, 0] \tag{4}$$

The subscript "m" represents the corresponding parameters in the porous medium. Here, μ_e is the effective viscosity which takes into account the slip at the interface between the porous surface and fluid together with the porosity. At the concentrations used, the CMC solutions also behave in a non-Newtonian manner with shear-thinning properties. However, since the model only considers the viscosity in a relatively stable range (near 10/s) in the present study, its non-Newtonian effect is limited.

The boundary conditions in this study are determined by considering the continuity of velocity and the shear stress at the interface, $u = u_m$ and $\tau = \tau_m$ at $y = 0$, as well as no-slip boundary conditions on the two plates, $u = 0$ at $y = 2L$ and $u_m = 0$ at $y = -2H$. Herein, we considered continuity of the tangential stress because Brinkman's equation has a viscous term which is similar to Navier-Stokes equation. Therefore, it is reasonable to assume that the tangential stress should be continuous along the interface[43,44].

To analyze a wider range of parameter changes in different subjects, we then normalized the length scales in both fluid and porous regions by *L* and *H*, respectively. Also, a constant pressure gradient is considered in the *x*-direction. Thus, Eq3 and Eq4 can be expressed as

$$\begin{cases} \dfrac{d^2 \tilde{u}}{d\tilde{y}^2} = C & \tilde{y} \in [0, 2] \\ \dfrac{M d^2 \tilde{u}_m}{\varepsilon \, d\tilde{y}^2} - \alpha^2 \tilde{u}_m = \dfrac{C}{d^2} & \tilde{y} \in [-2, 0] \end{cases} \tag{5}$$

$$M = \frac{\mu_e}{\mu}, \; \alpha^2 = \frac{H^2}{K}, \; d = \frac{L}{H}, \; C = \frac{L^2 \partial p}{\mu \, \partial x} \tag{6}$$

where $\tilde{u}$ and $\tilde{u}_m$ are the scaled velocity and $C = \frac{L^2 \partial p}{\mu \, \partial x}$ can be treated as a constant value which depends on the pressure gradient and geometry of each condition. M is the viscosity ratio (we

considered $M = 1$ in current study), α is the permeability parameter and d is the length ratio. Thus, the scaled shear stress in porous medium (tongue surface) can be expressed as

$$\tau_m = \frac{M\mu}{\varepsilon H}\left(\frac{\partial \tilde{u}_m}{\partial \tilde{y}}\right) \tag{7}$$

To determine the deflections of the papillae (Figure 3A), we assumed the papillae are distributed evenly, were subject to uniform shear stress in the simulated model, and the deflection is fairly small. The mechanical sensitivity would then be proportional to the amount of papilla deflection. As shown in Fig 3, let $z = y + 2H$, the deflection δ at x-axis direction of a single papilla can be obtained by solving the elastic curve equation

$$\frac{d^2\delta}{dz^2} = \frac{\overline{M}(z)}{EI(z)} \tag{8}$$

where $\overline{M}$ is the bending moment in the papilla, I is the moment of inertia of the cross section and E is Young's modulus, herein, we considered $E=2.6kPa$[16]. At an arbitrary height $z = \lambda$, the shear force caused by flow shear stress can be obtained as

$$F = \tau_m A \tag{9}$$

where A is the cross-section area at $z = \lambda$, and the moment $\overline{M}$ can be obtained as

$$\begin{cases} \overline{M}(z) = F \cdot (z - \lambda) & z \in [0, \lambda] \\ \overline{M}(z) = 0 & z \in [\lambda, 2H] \end{cases} \tag{10}$$

Thus, the max deflection can be solved computationally (more calculation details are shown in supporting information). Deflection was then correlated to PB JND to determine the relationship between proposed tip displacement and viscosity perception.

Finally, the model was used to help determine a potential minimum viscosity of relevance for this mechanism. As mentioned above, previous theoretical models used varied cutoffs ranging from 100-1000cPs[16,18] resulting in a minimum viscosity cutoff of 1000cPs for the psychophysical portion of this study. However, as both studies are theoretical, neither provides anatomical

14

support for the cutoff used. Thus, with the aim of determining a potential minimum viscosity where

this mechanism could be relevant, the calculated deformation at 5068cPs was used to find the

approximate viscosity needed to generate 1μm of tip deformation, an estimate of a potential

minimum deflection needed for transduction. Due to the unique anatomy of the papillae, with their

uncommon internal innervation and hair-like deformation there was no standard deflection cutoff[5].

We instead looked to other similar structures found throughout the body. Hair cells in the ear,

which also function based off fluid displacement, respond reliably to deformations as small as 2-

5nm[45], while cutaneous mechanoreceptors in glabrous skin may respond to deformations at or

below 5μm[46]. Other evidence suggests that mechanoreceptors surrounding hair follicles are

even more sensitive to hair deformation than the threshold reported for glabrous skin, but the

exact threshold has not been reported[47]. It is unlikely that the papillary structures are as sensitive

as the hair cells in the ear, but they are likely more sensitive than the glabrous skin due to the

unique geometry of the structures, thus an intermediate threshold of 1μm was chosen.

Results

Viscosity Discrimination

59 participants (age 19-40,18M/41F) were recruited via the Ohio State University

Consumer Sensory Database. Individuals with a self-reported history of an oral disease, food

allergies or sensitives, mobility problems that would prevent them from completing the physical

task, as well as smokers, were excluded. Individuals' Just-Noticeable-Difference (JND) thresholds

for high-viscosity solutions (η=4798-12260cP) in the oral cavity were determined using the

forced-choice staircase method[28,29] in two conditions: an Unblocked (UB) condition wherein

individuals evaluated solutions using their entire oral cavity and a Palate-Blocked (PB) condition

wherein individuals evaluated solutions with only their tongue while wearing a custom-molded

mouth piece to block their hard palate (Figure 1A and B). JND thresholds for viscosity were $\overline{\Delta\eta}$ =

1041.71cP ± 50.36cP for the UB condition and $\overline{\Delta\eta}$ = 1671.26cP ± 142.77cP for the PB condition;

these were significantly (p<0.00001) different. Sensitivity in the two conditions was not correlated (r=0.09, p=0.947).

Lingual Anatomical Characterization

For a subset of participants (n=44), a 5mm biopsy punch in the middle third of the dorsal tongue were collected under local anesthesia using forceps and scissors and analyzed using optical profiling with a Keyence VK-X210 Laser scanning confocal microscope (Figure 2A-C). The filiform papillary length, tip and base diameter, and density were measured and showed a greater diversity in size and shape than originally anticipated (see Supporting Information Figures S1A-D and S2A-C). Moreover, multiple different papillary phenotypes appear to be equally successful at discriminating between high-viscosity fluids. While average papillary length was 774.74μm ± 29.15μm, values ranged from 462.94μm to 1177.21μm with four individuals with averages below 500μm and four individuals with values over 1100μm. Average papillae length did not correlate with average base width (r= 0.133, p=0.385), tip width (r=0.0911, p=0.558) or average density (r=0.111, p=0.469), however the width and density themselves were slightly related (r= -0.298, p=0.047). When correlated to PB JND where only lingual mechanisms of viscosity perception were engaged, significant relationships were seen between length and PB JND (r=-0.581, p<0.0001, Figure 2D) and density and PB JND (r=-0.298, p=0.005, Figure 2E), with individuals with more, longer, papillae showing lower JNDs, translating to a higher acuity. However, papillary length and density vary independently, and it is the combined interaction of these variables that likely drive acuity. To capture this relationship, an individual's average papillary length was multiplied by their average papillary density to generate a "Papillary Score". This score was then correlated to PB JND and was found to have a more significant correlation than length or density alone (r=0.68, p<0.00001, Figure 2F). Base and tip diameter were not significantly correlated to psychophysical performance (r=-0.0314, p=0.921 and r=0.140, p=0.362, respectively).

Further investigation via multiple regressions analysis indicated that the significant filiform papillary attributes of length and density were not only strongly correlated to PB JND, but also

had a predictive relationship with an individual's acuity (Adj. R^2=0.433, p<0.001, Table 1).

Papillary length appeared to play the most significant role in predicting an individual's PB JND (β= -0.505, p<0.001), while density was also highly significant (β= -0.398, p=0.008). The other attributes tested in the model, papillary base and tip widths, age, and gender, were not found to have a significant impact on PB JND. Moreover, when all non-significant terms were removed, there was almost no loss of model-fit (Adj. R^2=0.431, p<0.001). Data here are in agreement with our hypothesis, suggesting viscosity perception on the tongue is significantly related to filiform papillary attributes.

Model Generation

Extending a previous study, the human tongue surface was modeled as a porous medium and the complex, high-viscosity Newtonian fluid flow through the papillae structures during the experiment was simulated. Papillary length, base and tip diameter, and density in each of the 44 human subjects was used to calculate the individual shear stress exerted onto the tongue surface and papilla structure by the viscous solution. The key parameters of the porous medium—permeability and porosity— were estimated based on well-established theoretical formulae[38–40]. An elastic curve equation was applied to predict filiform papillae deformation as a function of viscous shear stress (Figure 3A).

Results from the model simulation of papillary deformation indicated that the degree of predicted tip displacement (δ_{max}) was particularly affected by papillary length and density and was highly significantly (r=0.736, p<0.00001) correlated to the Papillary Score (Figure 3B). Individuals with more, longer structures had greater fluid-structure interactions with the viscous fluids which can explain the observed increase in modeled papillae displacement. When comparing this modeled displacement to the observed PB JNDs, there was a significant correlation (r=-0.470, p<0.001) with individuals with greater predicted displacement generally having lower JNDs (Figure 3C). There is notably no linear relationship between papillary tip or base diameter and calculated deformation (r=0.051, p=0.586), and instead, a more parabolic one. The model indicated this is likely due to a reciprocal interaction between papillae diameter and fluid shear

17

stress. Papillae with larger diameters would result in higher viscous shear stress due to a narrower gap and stronger fluid-structure interaction, but larger-diameter papillae would also deform less easily, thus their effects canceling each other. Using this deformation data, we were also able to determine a minimum viscosity for deformation which could potentially translate to a minimum viscosity where this mechanism could become relevant for perception. As anticipated these viscosity values were highly variable and dependent upon papillary geometry, ranging almost tenfold (183.921-1487.698cP) with an average threshold of 604.102 ± 55.777cP. Thresholds skewed lower, with a greater proportion of individuals with a threshold below 500cP (median 495.532cP, See Supporting Information Figure S3).

Discussion

The elevated JND in the PB condition appears to suggest that the tongue is not solely responsible for high-viscosity solution perception. At the individual level, this point is further underscored by the lack of correlation between the two conditions suggesting that while some individuals rely heavily upon their tongues for solution discrimination, others may instead rely more heavily on other oral tissues. A similar phenomenon was observed when assessing sphere size using the tongue. Engelen, et al. (2002) found that the palate hindered the estimation of the size of large (4-9mm) spheres (attributed to a limited contact area between the sphere and the hard palate) when compared to evaluation with the tongue alone [32]. Here instead it appears that the palate may have an additive effect in viscosity perception that still works independently of the papillary amplification mechanism on the tongue. While this is likely due to mechanosensory contributions coming from the palate, it may also be due, in part, to the smoothed geometry of the PB mouthpiece which may dampen on-tongue perception without the presence of rugal prominences for the papillae to press against. While palate surface geometry has not been found to be relevant for other lingual textural percepts, the geometry has been shown to be critical for speech[48,49]. As such, these findings highlighted the importance of the decision to compare

18

papillary traits to the PB JND values, not UB JND ones. Only in the blocked condition, wherein the other tissues are removed, can a structure-specific mechanism truly be evaluated.

Still, it is challenging to compare JND values obtained here to values reported previously for two reasons. First, with the low viscosities and differential evaluation techniques (i.e. swishing in the mouth, swallowing, spitting, etc.) used in other studies, it is unlikely that the same perceptual mechanism proposed here is being utilized[16,50]. Aside from the passive flow described above, in these instances, information may be gleaned via the muscular force required to push the tongue through the solution or around the mouth (swishing), via difficulty of swallow or esophageal cues post-swallow (swallowing), or via force required to spit the solution or cues from the lips during expectoration (spitting)[10,12,16]. Additionally, prior studies[10,12,13,15,17] primarily relied on magnitude estimation, a method which is more suited for suprathreshold studies due to its inability to resolve the small perceptual differences inherent to threshold tasks[10,12,14]. As such, in this study, we utilized the forced-choice, staircase method, which enabled us to complete a threshold-level assessment of sensitivity and gain insight into detection mechanisms more directly. Thus, the psychophysical curves generated in these previous studies likely do not apply here as they do not reflect the same mechanism nor describe the same psychophysical percept.

From what limited data is available for threshold assessments using the tongue-pressing evaluation technique, Steele, et al. (2014) found that a 0.67-fold increase in viscosity was required for reliable solution discrimination in a triangle test task for xanthan gum solutions ranging in viscosity from 710-1580cP at 10°C when evaluated with the tongue and palate[14]. However, the authors acknowledge the solutions were likely lower in viscosity during the evaluation due to the temperature dependent nature of xanthan gum over their tested concentrations[51]. This value is much higher than the average 0.21-fold viscosity increase needed for discrimination obtained here. There are potentially multiple reasons for this difference. First, the non-directional triangle test lacks power due to the unknown nature of the difference presented which may have resulted in poorer discrimination[52]. It is also possible that the differential shear thinning imparted by xanthan gum – as opposed to the CMC/glycerol system

used here – resulted in a more difficult comparison. Finally, due to the thinner viscosities in the Steele, et al. (2014) study, a different physiological mechanism may underpin the viscosity assessments made by subjects during that evaluation task. Based on the proposed viscosity cutoffs for the papillary mechanism from our model, the solutions tested by Steele, et al. may fall into a range where evaluation is completed via different mechanisms dependent upon an individual's papillary traits. Moreover, some individuals may transition between evaluation mechanisms (i.e., passage rate through the mouth to papillary deformation) in this range which may also help to explain the larger increase in viscosity needed for discrimination.

Lingual Anatomical Characterization

While viscosity perception in the oral cavity appears to be more multifaceted than originally hypothesized, anatomical characterization does appear to suggest that the perception of high-viscosity solutions on the tongue is related to the filiform papillary attributes of length and density, but this perception is most significantly related to the interaction of these two traits (Figure 2D-F). This is to say, that individuals with more, longer papillae, appear to be better at differentiating between viscous solutions than individuals with fewer, squatter structures. Moreover, multiple regression analysis finds that variation in PB JND can be predicted using these papillary attributes alone (Table 1). Papillary length appears to be the most relevant attribute and can also serve to explain individuals with unusually high or low JNDs for their density. For instance, in two individuals with approximately equivalent papillary densities (8 vs 8.38), their PB JNDs differed greatly. The first individual had a much higher JND than anticipated (JND = 3874.63cP), while the second had a much lower one (JND = 488.00cP). When looking at the average papillary length for these individuals, however, the cause of their extreme nature becomes apparent. The first individual had a very short average papillary length (Avg. length = 462.95µm), while the second had a much higher average (Avg. length = 905.24µm). This points to the idea that density may not be relevant when structures are too squat to deform or, if innervation is below and not within the papillae, potentially too small to generate sufficient strain on the tongue's surface for signal transduction. Similarly, if structures are long enough, fewer may

be needed to generate a large enough signal for perception to occur. This effect further underscores the necessity of the "Papillary Score" metric which factors in both relevant attributes simultaneously.

It is also important to note that sample analysis via optical profiling also indicated a larger degree of variance in papillary shape and size than suggested by previous work (Figure S1A-D and Figure S2A-C)[22,24], however, there was little variation within a given individual. While values were not as low as the 250μm proposed in the modelling papers, structures ranged in average length by over 600μm (Figure S1A-D) [16,18]. This degree of variation present may explain the inconsistencies in the values previously reported in anatomical studies[23,24]. Additionally, there does not appear to be a specific, optimal papillary geometry that is more or less sensitive to these viscosity differences (Figure S2A-C). However, future investigation into additional papillary attributes including hair-like projection length and number, as well as overall papillary rigidity may provide further insight into this mechanism. Regardless, the confirmation of the mechanosensory relevance of the filiform papillary structures in viscosity points to their potential relevance in other textural percepts.

Model Generation

Characterizing sensory acuity without consideration of a proposed mechanism provides only descriptive insights. By contrast, prior models of filiform displacement underpinning viscosity perception were entirely theoretical and did not leverage anatomical or sensory data into their development[16,18]. Presently, we used anatomical data as inputs to successfully model the human tongue surface as a porous medium and simulated the complex, high-viscosity, Newtonian fluid flow through the papillae structures. This simulation enabled the prediction of filiform papillae deformation as a function of viscous shear stress, and we show that degree of deformation is strongly associated with viscosity sensitivity in humans.

Insights from the generated tip displacement model also help to explain the findings of the anatomical characterization. The significant correlation between proposed displacement and the papillary score indicates that individuals with more, longer papillae should see a greater tip

displacement (Figure 3B). Moreover, the significant relationship with PB JND and displacement also indicates that these individuals who do see greater displacement at lower forces are generally better at discriminating viscosity on the tongue (Figure 3C). However, deformation only explains approximately 22% of the variance seen in the JND. This effect is likely because of underlying assumptions of the model such as a constant Young's modulus for all individuals. Moreover, differences in innervation density and neural signaling are also challenging to measure, and thus not factored in. Importantly, however, the displacement model does help to explain the lack of significant relationship between papillary width and PB JND, a finding that was unanticipated. The model suggests that papillae with larger diameters result in higher viscous shear stress due to a narrower gap and stronger fluid-structure interaction, but a larger-diameter papilla also deforms less easily when compared to more average structures (see supporting information). Similarly, however, structures with smaller cross-sectional areas result in a lower viscous shear stress, and thus less deformation.

Results from the model were also used to determine a potential minimum viscosity for this evaluation mechanism. As anticipated, the differences in papillary dimensions resulted in a variable threshold ranging from 183.921cPs (somewhat near the value chosen by Lauga et al.), and 1487.698cPs (well above the 1000cPs cutoff proposed by van Aken) (Figure S3)[16,18]. Individuals with more numerous, longer structures, generally had lower thresholds, suggesting that the mechanism may become relevant for much thinner solutions. Future studies investigating discrimination of lower viscosity solutions (~100cP<η<1500cP) in this transitional range should account for this potential change in evaluation mechanism in their study design. It is also important to acknowledge the current limitations and assumptions made as part of the current model. As this is an initial study to explore the correlation between mechanical stress and sensory perception, a 2D, steady-state, shear flow model was chosen as it is a good initial approximation of a cross-sectional path of a 3D elongational flow. In the future, the model can be improved to incorporate time-dependent 3D elongational squeeze-flow effects as well as more

realistic representation of the tongue squeeze force. The future addition of individual-specific

fungiform papillary attributes may also further tailor the model.

Finally, by understanding the filiform papillae's relevance in viscosity perception we may

also gain insight into a reason for decreased viscosity perception that has been observed with

aging[27]. Kobayashi, et al. (2001) found significant degradation of filiform papillary cores in tongue

samples taken from the cadavers of older adults (Age>60)[53]. Compared to samples from younger

individuals, whose structures were similar to those described in the present study, older adults'

tongues had higher rates of filiform papillary hair loss and complete filiform papillary loss.

Additionally, filiform cores were also shown to fuse in older adults, resulting in larger structures

with fewer hair-like protrusions. Based on the data seen above, it is possible that fusion could

lead to a decrease in structural deformability, and thus a decrease in viscosity perception ability.

Moreover, if the denuding and hair-loss described is due to aging-related degradation of papillary

structures, it may also help to explain the decrease in tactile acuity previously observed. Future

studies into papillary changes related to aging and their impacts on high-viscosity perception

would be needed to confirm this link.

Conclusions

Despite the abundance of claims implicating filiform papillae in mechanosensation, no

prior study has provided psychophysical evidence supporting their role. The present investigation

is the first to confirm that the perception of high-viscosity solutions on the tongue is likely related

to the deformation of the filiform papillae. Additionally, we have provided a deformation model for

filiform papillae as perceptive structures that has been informed and tested with psychophysical

data. Moreover, this study also provides the first psychophysical and anatomical evidence for a

mechanistic explanation of a textural percept on an oral soft tissue. However, these findings also

serve to highlight the fact that the deformation of the filiform papillae is likely not the sole

mechanism of oral viscosity perception. Instead, other tissues, such as the palate and gums, may

also be involved.

Author contributions

C.T.S. and B.L.M. conceived the project, worked to develop the experimental design, and write the manuscript. K.S.K. developed the biopsy protocol, executed all lingual biopsies, and edited the manuscript. K.Z. and Z.W. developed and executed the deformation model from the data and helped to write and edit the relevant portions of the manuscript. B.L.M. developed testing solutions, performed psychophysical experiments, collected anatomical measurements, and analyzed data. C.T.S. supervised the research.

Compliance and ethics

Human subjects protocols (2013B0277, psychophysical protocol and 2018H0509, biopsy protocol) were approved by the Ohio State University Institutional Review Board. All procedures followed the guidelines from the Declaration of Helsinki for medical research using human subjects.

Conflicts of interest
There are no conflicts of interest to declare.

References

1   V. L. van Stokkom, A. E. Blok, O. van Kooten, C. de Graaf and M. Stieger, *Appetite*, 2018,

121, 69–76.

2   D. Kilcast and D. F. Lewis, *Nurtition Bull.*, 1990, **15**, 103–113.

3   C. L. Scott and R. G. Downey, *J. Psychol. Interdiscip. Appl.*, 2007, **141**, 127–134.

4   Y. Moayedi, L. F. Duenas-bianchi and E. A. Lumpkin, *Nat. Sci. Reports*, 2018, **8**, 1–14.

5   Y. Moayedi, E. A. Lumpkin, M. Park and A. Koch, *J. Comp. Neurol.*, 2021, **529**, 3046–3061.

6   F. Moehring, P. Halder, R. P. Seal and C. L. Stucky, *Neuron*, 2019, **100**, 349–360.

7   M. Trulsson and G. K. Essick, *J Neurophysiol*, 1997, **77**, 737–748.

8   M. Trulsson and G. K. Essick, *J. Neurophysiol.*, 2010, **103**, 1741–1747.

9   P. Haggard and L. De Boer, *Neurosci. Biobehav. Rev.*, 2014, **47**, 469–484.

10   C. M. Christensen and L. M. Casper, *J. Food Sci.*, 1987, **52**, 445–447.

11   F. Shama and P. Sherman, *J. Texture Stud.*, 1973, **4**, 102–110.

12   C. H. Smith, J. A. Logemann, W. R. Burghardt, S. G. Zecker and A. W. Rademaker, *Dysphagia*, 2006, **21**, 209–217.

13   C. M. Christensen, *J. Texture*, 1979, **10**, 153–164.

14   C. M. Steele, D. F. James, S. Hori, R. C. Polacco and C. Yee, *Dysphagia*, 2014, **29**, 355–364.

15   C. C. Elejalde and J. L. Kokini, *J. Texture Stud.*, 1992, **23**, 315–336.

16   G. a. van Aken, *Soft Matter*, 2010, **6**, 826.

17   J. L. Kokini, J. B. Kadane and E. L. Cussler, *J. Texture Stud.*, 1977, **8**, 195–218.

18   E. Lauga, C. J. Pipe and B. Le Révérend, *Front. Phys.*, 2016, **4**, 1–8.

19   A. C. Noel and D. L. Hu, *J. Exp. Biol.*, , DOI:10.1242/jeb.176289.

20   R. G. Bangcuyo and C. T. Simons, *Exp. Brain Res.*, 2017, **235**, 2679–2688.

21   G. K. Essick, A. Chopra, S. Guest and F. Mcglone, 2003, **80**, 289–302.

22   M. Manabe, H. W. Lim, M. Winzer and C. A. Loomis, *Arch. Dermatol.*, 1999, **135**, 177–81.

23   K. Kobayashi, M. Kumakura, H. Shinkai and K. Ishii, *Acta Anat. Nippon*, 1994, **69**, 624–635.

24   A. Kulla-Mikkonen and T. E. Sorvari, *Acta Anat. (Basel).*, 1985, **123**, 114–120.

25   Z. Wu and K. Zhao, *PLoS Comput. Biol.*, 2020, **16**, 1–13.

26   X. H. Yang and W. L. Zhu, *Cellulose*, 2007, **14**, 409–417.

27   C. M. Steele, L. Hill, S. Stokely and M. Peladeau-Pigeon, *J. Texture Stud.*, 2014, **45**, 317–323.

28   B. Linne and C. T. Simons, *Chem. Senses*, 2017, **42**, 525–535.

29   B. L. Miles, K. Van Simaeys, M. Whitecotton and C. T. Simons, *Physiol. Behav.*, , DOI:10.1016/j.physbeh.2018.07.002.

30   A. N. Cutler, E. R. Morris and L. J. Taylor, *J. Tex*, 1983, **14**, 377–395.

31   L. Engelen, A. Van Der Bilt, M. Schipper and F. Bosman, *J. Texture Stud.*, 2005, **36**, 373–386.

32   L. Engelen, J. F. Prinz and F. Bosman, *Arch. Oral Biol.*, 2002, **47**, 197–201.

33   D. R. Riskey, J. A. Desor and D. Vellucci, *Chem. Senses*, 1982, **7**, 143–152.

34   B. L. Miles, K. van Simaeys, M. Whitecotton and C. T. Simons, *Physiol. Behav.*, 2018, **194**, 515–521.

35   T. M. Nuessle, N. L. Garneau, M. M. Sloan and S. A. Santorico, *J. Vis. Exp.*, 2015, **100**, 1–9.

36   W. J. Hume and C. S. Potten, *J. Cell Sci.*, 1976, **22**, 149–160.

37   S. Iwasaki, H. Yoshizawa and I. Kawahara, *Acta Anat. (Basel).*, 1996, **157**, 41–52.

38   G. W. Jackson and D. F. James, *Can. J. Chem. Eng.*, 1986, **64**, 364–374.

39   M. Agelinchaab, M. F. Tachie and D. W. Ruth, *Phys. Fluids*, 2006, **18**, 017105.

40   R. Crawford, G. F. Jones, L. You and Q. Wu, *Chem. Eng. Sci.*, 2011, **66**, 294–302.

41   D. Jasikova, M. Kotek, S. Fialova and V. Kopecky, *WSEAS Trans. Biol. Biomed.*, 2017, **14**, 83–88.

42   H. C. Brinkman, *Appl. Sci. Res.*, 1949, **1**, 27.

43   N. S. Martys and J. G. Hagedorn, *Mater. Struct.*, 2002, **35**, 650–658.

44   I. Battiato, P. R. Bandaru and D. M. Tartakovsky, *Phys. Rev. Lett.*, 2010, **10**, 1144504.

45   A. Fridberger, I. Tomo, M. Ulfendahl and J. B. De Monvel, *Proc. Natl. Acad. Sci.*, 2006, **103**, 1918–1923.

46   A. Iggo and H. Ogawa, *J. Physiol.*, 1977, **266**, 275–296.

47   B. Y. A. G. Brown and A. Iggo, *J. Physiol.*, 1967, **193**, 707–733.

48   C. A. Gitto, S. J. Esposito and J. M. Draper, *J. Prosthet. Dent.*, 1999, **81**, 237–239.

49   A. Tanaka, Y. Kodaira, K. Ishizaki and K. Sakurai, *J. Oral Rehabil.*, 2008, **35**, 715–721.

50   T. Aktar, J. Chen, R. Ettelaie and M. Holmes, *J. Sens. Stud.*, 2015, **30**, 98–107.

51   W. A. Al-Masry, N. M. Ghasem, K. A. Al-Sugair and A. Ibrahim, *J. Saudi Chem. Soc.*, 2005, **9**, 197–202.

52   S. McClure and H. T. Lawless, *Food Qual. Prefer.*, 2010, **21**, 547–552.

53   K. Kobayashi, M. Kumakura, K. Yoshimura and J. Shindo, *Ital. J. Anat. Embryol.*, 2001, **106(Suppl)**, 305–311.
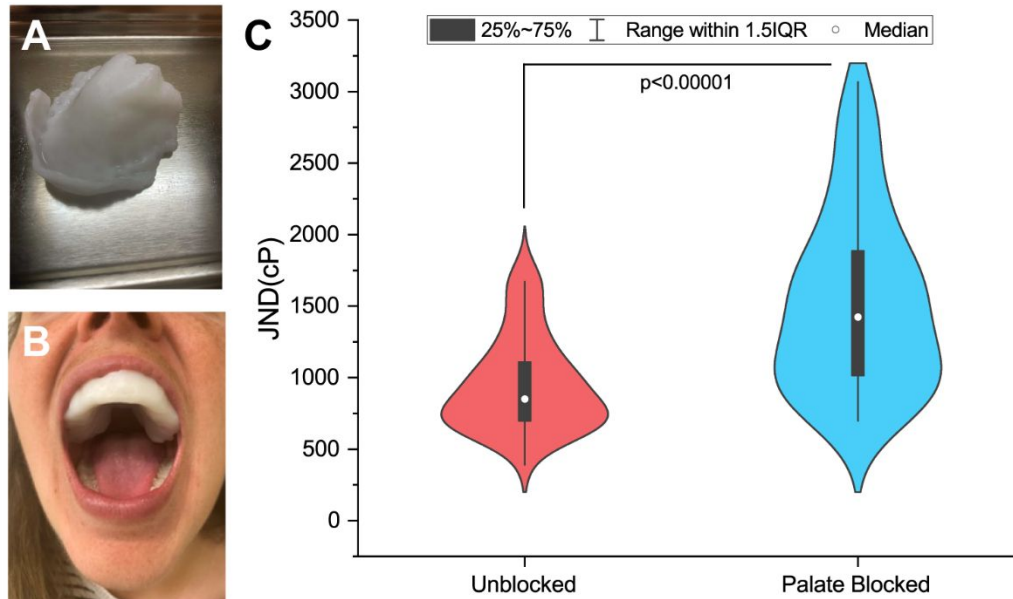
Figures and Tables

Figure 1A-C: Average Viscosity JNDs for the oral cavity and isolated tissues. Participants (n=59) evaluated solutions in two treatment conditions: an Unblocked (UB) condition where evaluation was completed with the tongue and palate, a Palate-Blocked (PB) condition where participants wore a molded, plastic mouth piece (A&B) and evaluated using only their tongue. Just-Noticeable-Difference (JND) thresholds were calculated for all participants and compared using a paired samples t-test. Individuals were significantly better (p<0.00001) at discriminating between viscosities in the Unblocked condition (JND=1041.71cP±50.36cP) than in the Palate Blocked condition (JND=1671.26cP±142.77cP, C)
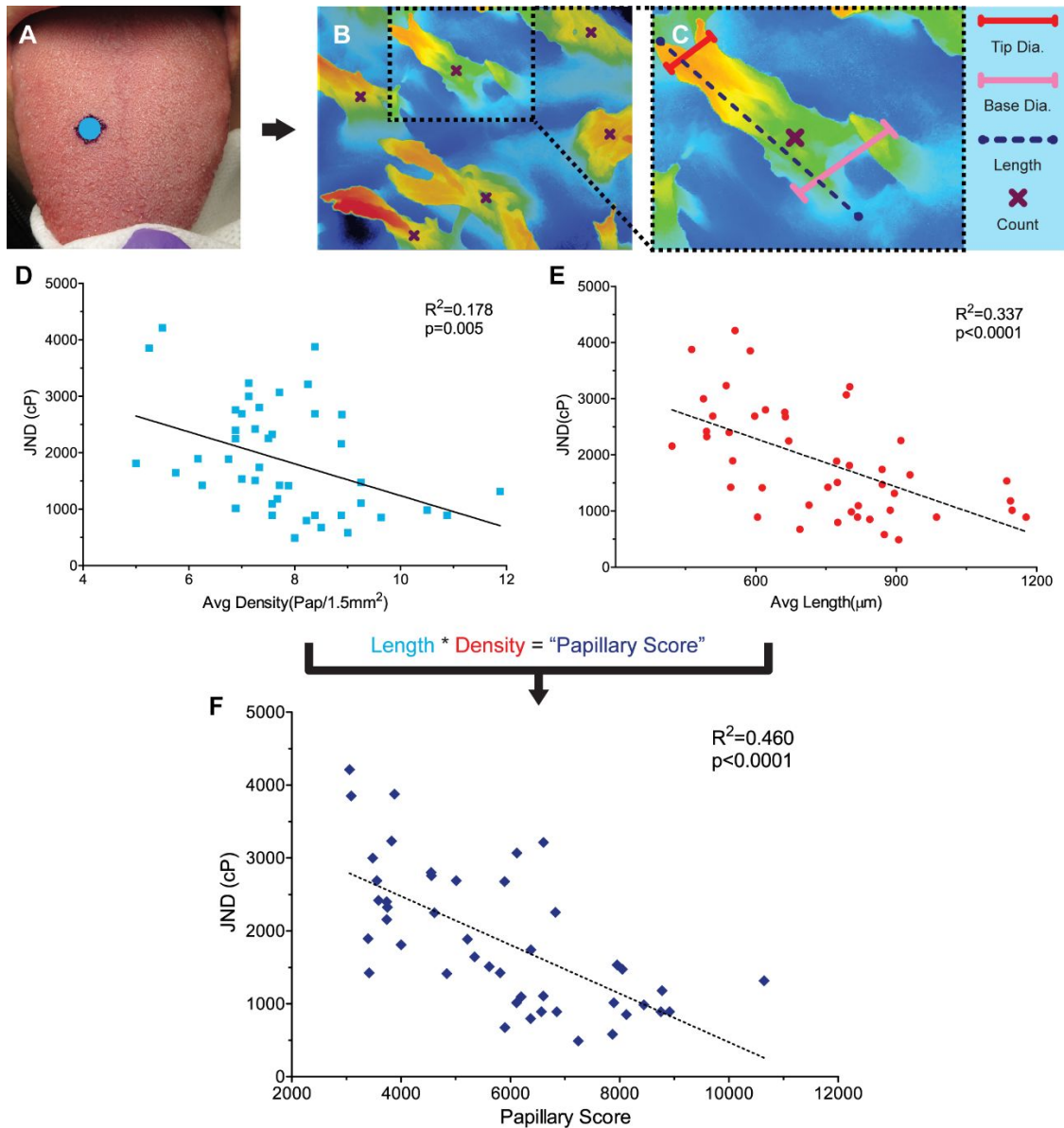
Figure 2A-F: Linear correlation of filiform papillary attributes with average Palate-Blocked JND. 5mm punch biopsies were taken from the dorsomedial tongue (A) and imaged using an optical profiler (B&C). Average tip diameter, base diameter, length, and count per image (density) were measured (B&C) for a subset of participants (n=44) and correlated to Palate-Blocked (PB) JND. Average papillary length and density were significantly correlated to JND (p<0.0001 and p=0.005, D&E, respectively), but papillary tip and base diameter showed no significant correlation (p=0.362 and p=0.921, respectively). To better capture an average representation of how many

structures of what length were present on the tongue density and length were then multiplied for each participant to generate a "Papillary Score", PB JND was compared to this score using a linear correlation and found to be highly significant (p<0.00001) and more significantly related to PB JND than length or density alone (F).

Table 1: Multiple regressions model of variation in Palate-Blocked JND. A multiple linear regression was completed utilizing all collected variables to assess their relative contributions to variation in PB JND. The regression was highly significant (p<0.0001). Average papillary length and papillary density were both significant drivers of variation (p<0.001 and p=0.008, respectively). Average papillary base and tip width, age, and gender were not significant.

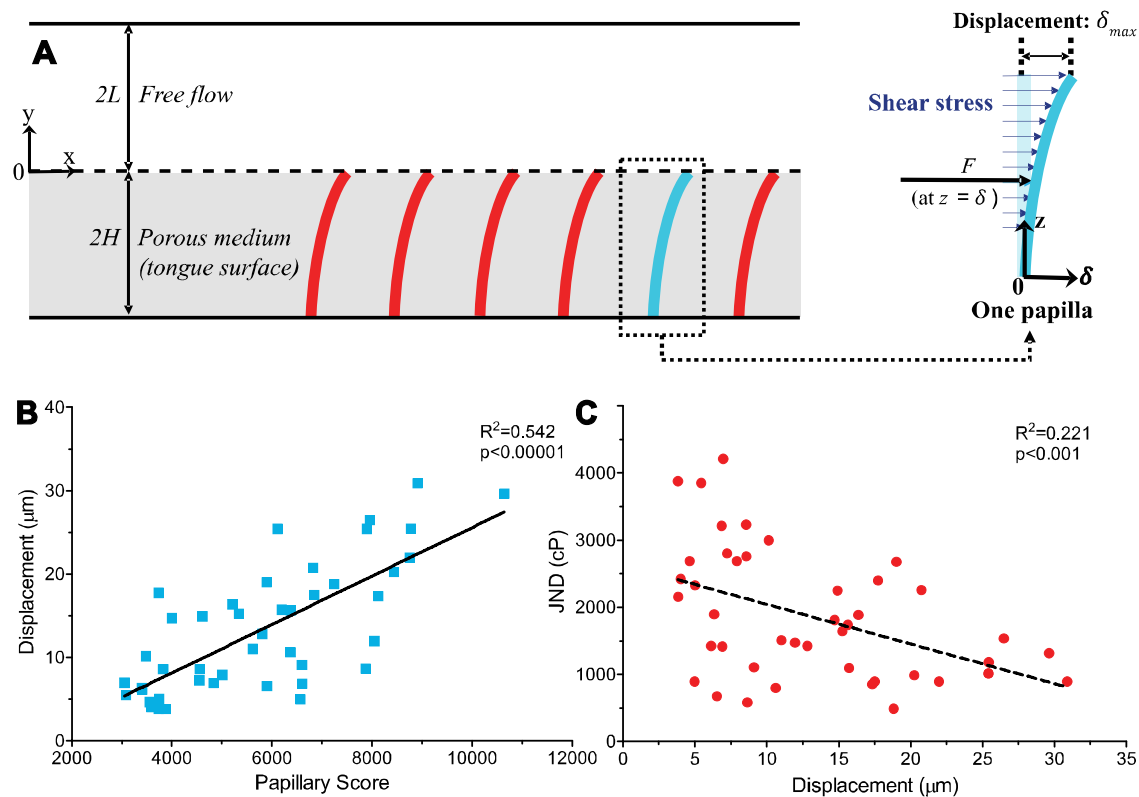| Model*	Unstandardized Coefficients		Standardized Coefficients	t	p-value
	B	Std. Error	β		
(Constant)	7117.949	1704.783		4.175	<0.001
Pap. Length	-2.447	0.598	-0.505	-4.092	<0.001
Pap. Density	-270.263	95.943	-0.398	-2.817	0.008
Pap. Base Width	-1.049	2.352	0.062	-0.446	0.658
Pap. Tip Width	0.097	2.718	0.006	0.036	0.972
Age	-17.596	27.273	-0.085	-0.645	0.523
Gender	-371.751	265.308	-0.189	-1.401	0.169

*p<0.0001, Adj. R^2=0.433

Figure 3A-C: Linear correlations of psychophysical attributes and simulated displacement.

Displacement was modeled using a solution with a viscosity of 5860cPs for all individuals by treating the papillae as elastic conical frusta distributed across the tongue's surface (A). The free flow condition (2L) represents the space between the tongue and hard palate or plastic mouthpiece, and the porous medium (2H) represents the surface of the tongue covered by papillary bodies. Force at height z is equivalent to the product of shear stress through the porous medium and the cross-sectional area at that height. In turn this leads to displacement δ_{max} at the tip of the structure. Papillary score was highly-significantly correlated ($p<0.00001$) to predicted displacement (B). Individuals' PB JND was also significantly related ($p<0.001$) to the proposed tip displacement (C).